

# High-resolution velocity model estimation by the RTH method

*Gennady Erokhin\* and Vitaliy Bryksin*

# Introduction

Some words about background and history of researches. The main idea of optical holography is based on the fixing the amplitude and phase of the wave scattered by object. The mechanism of such fixing uses the interference between scattered wave and some reference wave. It is so called two beams interferometry. The interference is "frozen" by a photographic plate, used later when creating a holographic image (Gabor, 1948).

Over 40 years ago, the ideas of optical holography were actively used when trying to create new mathematical methods for seismic data processing (Fitzpatrick et al., 1972).

As the result, during these way, such methods as Kirchhoff depth migration, Reverse Time Migration (RTM) (Baysal et al., 1983; McMechan, 1983) and Full Wave Inversion methods (Tarantola, 1984; Virieux, et al., 2009) were have been developed.

Until now, some researchers continue to consider that, in a sense, seismic data is seismic holography (Robinson et.al, 2010). I am agree with them. And so the method Reverse Time Holography (RTH) allows embodying the idea of optical holography to seismic data processing workflow (Erokhin et al., 2017, 2018a, 2018b; Erokhin, 2019).

Of course the RTH approach requires more computational power than the conventional RTM-based methods, but It provides research on the structural, geological, and petro physical properties of medium at a new qualitative and quantitative level

# Method

The velocity estimation of the medium and other seismic attributes by the Reverse Time Holography (RTH) method is carried out in two stages: ***Decomposition*** and ***Synthesis***.

The **first stage** of the RTH -decomposition consists in the development of some Vector Domain Common Image Gathers dataset (VDCIG). The creation of the VDCIG's repository is based on the full vector decomposition of two vector fields: direct and reversed in time (Erokhin et al., 2018a) for each 3D voxel (or 2D pixel) of the medium. There exist some conventional approaches for decomposition of forward and backscattered acoustic fields which use only pressure fields. The angles of incident and scattered waves are calculated using, for example, the Pointing vector (Yoon and Marfurd, 2006), which is accumulated on time. The RTH's VDCIG data power is significantly greater than the data power of conventional RTM or Angle Domain RTM methods.

# RTH data processing workflow

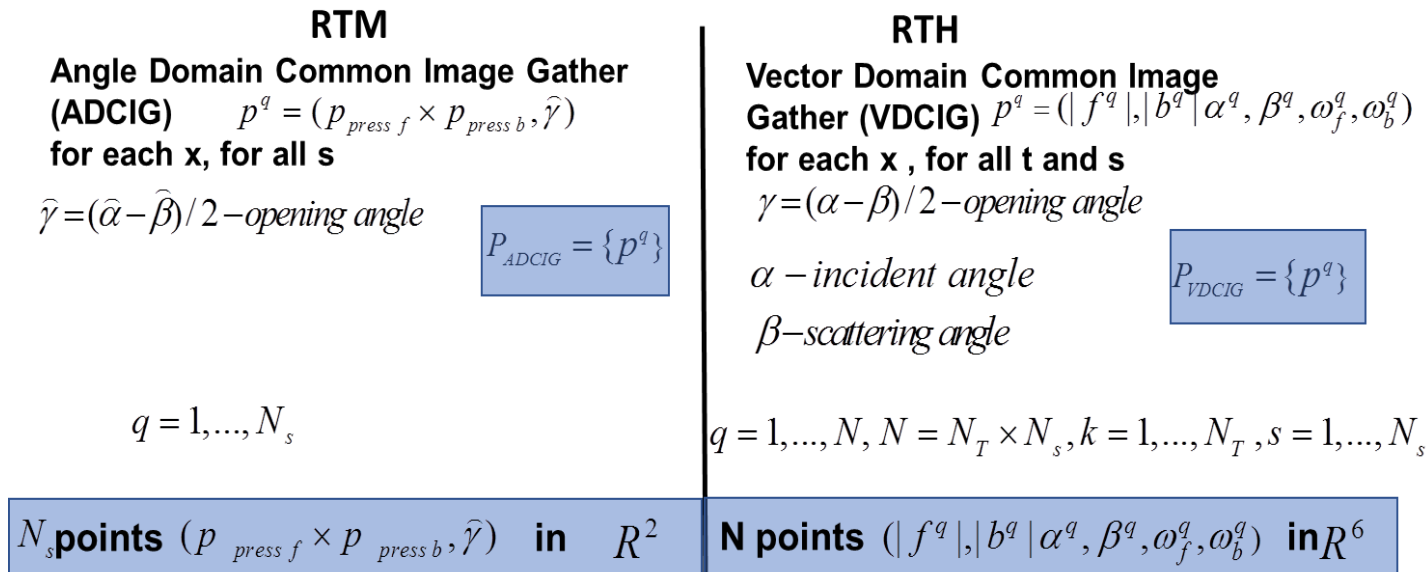


Figure 1: Data power comparison of RTM and RTH

Here  $\omega_f, \omega_b$  are the instantaneous circular frequency of rotation of forward vector  $f$  and backscattering vector  $b$  (Hz, clockwise positive, versus negative).

# RTH data processing workflow

The **second stage** of the RTH approach is to synthesize an attributes based on the parameters evaluation for the VDCIG dataset. For this purpose we use the statistical estimation of the multidimensional distribution. The workflow of the RTH data processing is presented at Fig. 2.

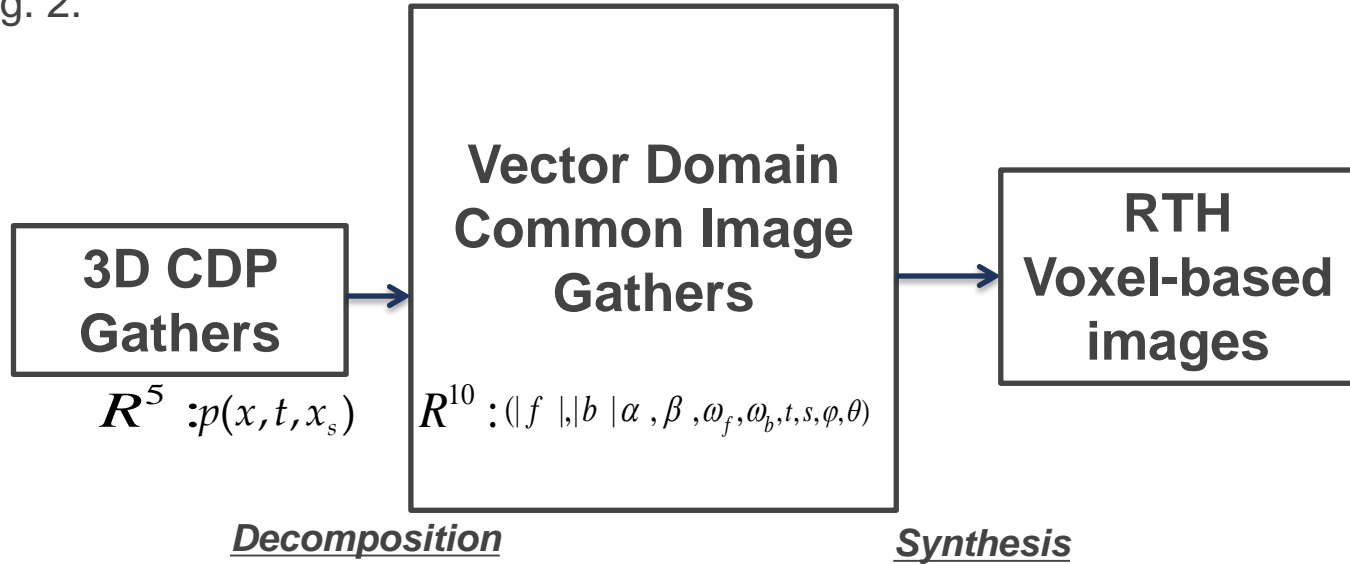


Figure 2: The RTH data processing workflow

Here  $t$  - time,  $s$  - parameter source,  $\varphi$  - azimuthal angle,  $\theta$  - polar angle

# Mathematical modelling

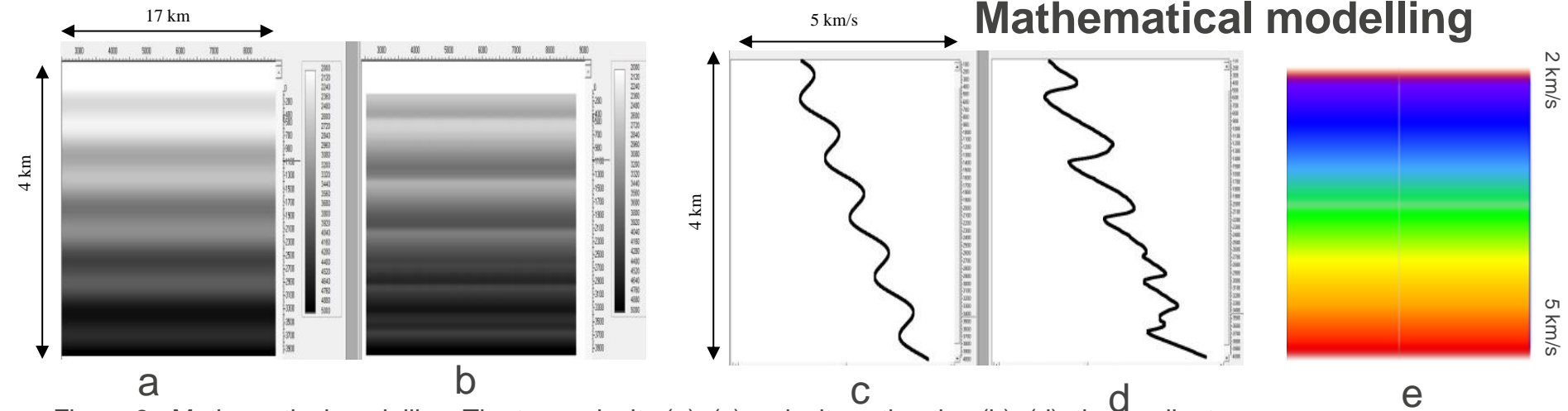


Figure 3: Mathematical modelling. The true velocity (a), (c), velocity estimation (b), (d), the gradient initial velocity model from 2 km/s (blue) up to 5 km/s (red) (e)

One of the parameters, estimated by VDCIG for each voxel of the medium (pixel for 2D case) is the perturbation value of arrival time regarding to background velocity. It turns out that the RTH method allows one to estimate the velocity in the medium through a perturbation of the arrival time in each voxel of the medium. The voxel size can be anything from 1-2 meters. Fig. 3 shows the result of velocity estimation (Fig. 3b, 3d) for the test with wavy velocity model (Fig. 3a, 3c). The voxel size is 5x5 meters, step between receivers is 25 m, between sources - 50 m and the number of sources is 344. Background velocity is simple gradient from 2 km/s up to 5 km/s (Fig. 3e).

# Comparison the RTH velocity and the logging data

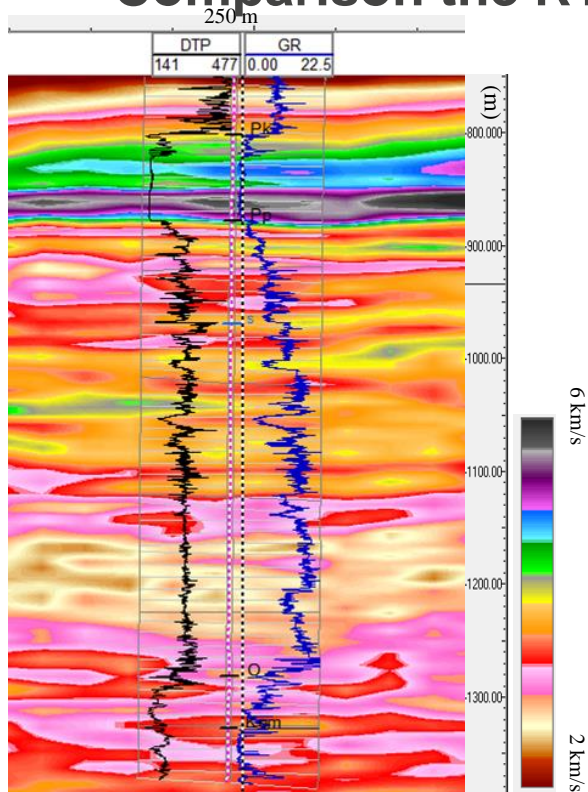


Figure 4: Comparison the RTH velocity and the logging data. Baltic syncline.

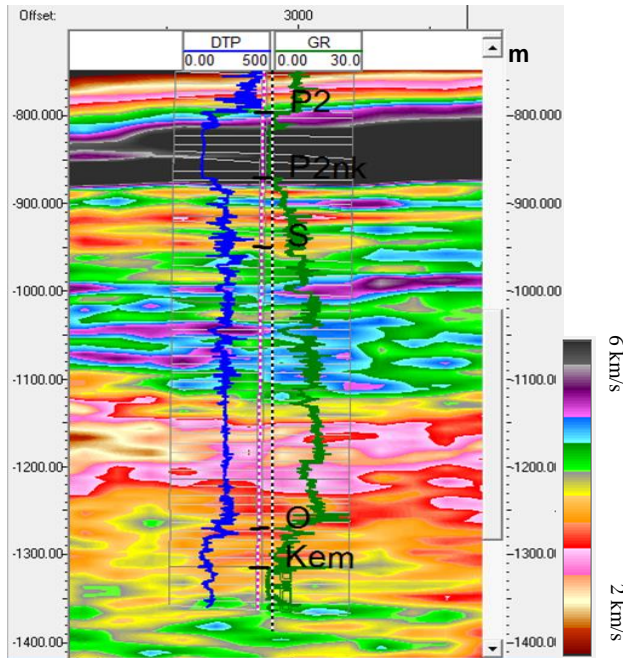
Except mathematical modeling correctness of the attributes, obtained on the basis of the RTH method also is confirmed in practice by geological information, including logging data.

Comparison of the RTH velocity with the logging data is presented at Fig. 4. Here the voxel size is 25 m lateral and 5 m deep.

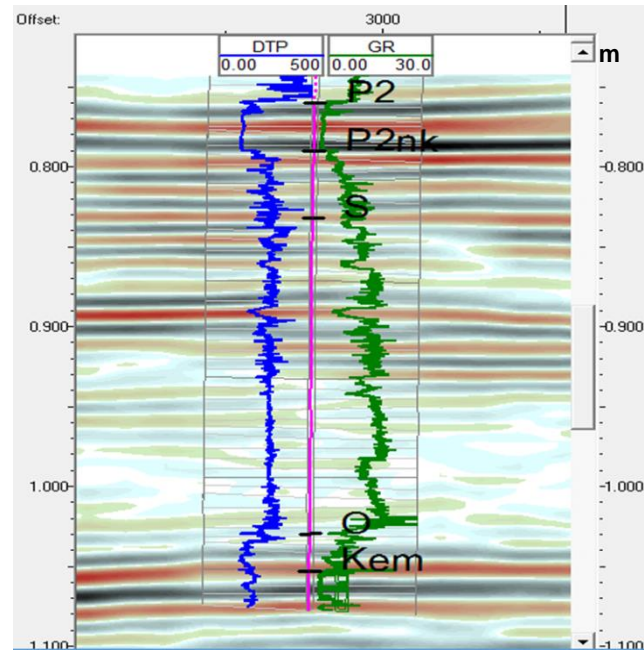
At depths of 800–900 meters, the anomalies of RTH velocity and of the logging are observed due to the high-velocity Permian deposits (Pk-Pp).

The principle difference between constructing RTH attributes from those obtained traditionally consists in their complete independence from each other and the possibility simultaneous creation all of them for each voxel of acoustic medium.

# Comparison of RTH velocity with conventional PSTM



RTH Velocity



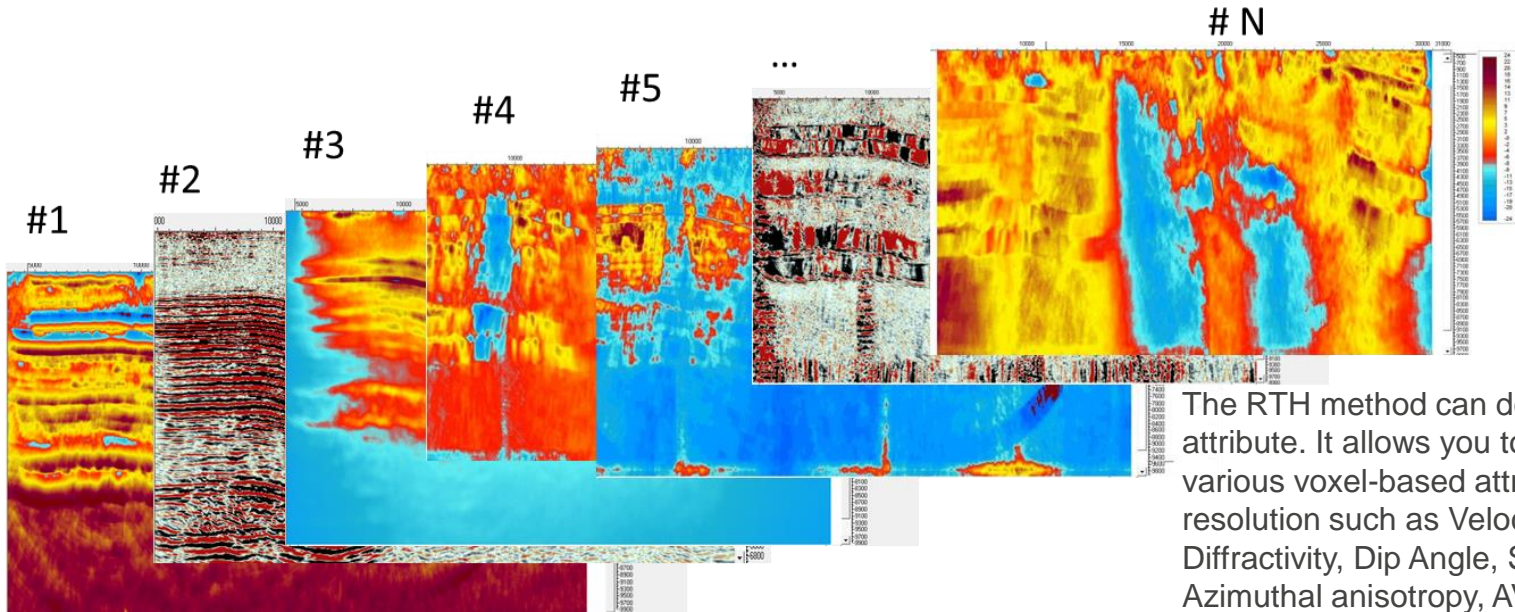
PSTM

Figure 5: Comparison of RTH velocity with PSTM. Dark color palette - Perm high velocity deposits. Baltic syncline.



# About RTH attributes

RTH attributes are calculated from VDCIG data and form a vector of length  $N$  ( $N > 20$ ) in each calculated voxel



The RTH method can design not only velocity attribute. It allows you to simultaneously obtain various voxel-based attributes of high spatial resolution such as Velocity, Reflectivity, Diffractivity, Dip Angle, Scattering Anisotropy, Azimuthal anisotropy, AVO, etc.

# Voxel-based classification of seismic imaging methods

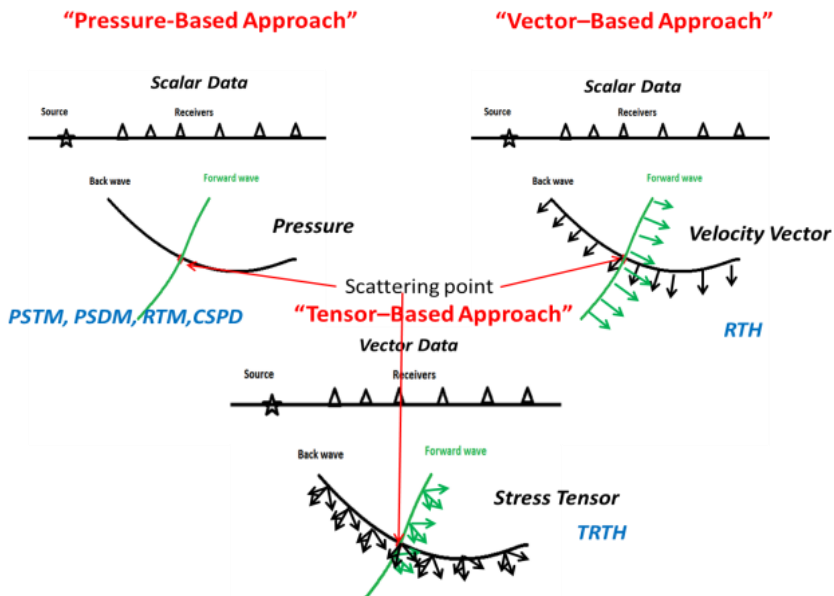


Figure 6: New voxel-based classification of the seismic imaging methods

Based on the RTH-approach we can design a new voxel-based classification of all seismic imaging methods. From the point of view of the mechanism for creating seismic images, the RTH method has a fundamental difference from all previous methods of time and depth migration, such as Kirchhoff migration, PSTM, PSDM, RTM, CSPD, etc.

This difference is concluded in other - statistical principles of imaging of scattering medium.

The new voxel-based classification of the seismic imaging methods is based on the next principals:

- If a method operates only with amplitude of wave for image of properties at each voxel of medium, then it can be called **scalar-based method** (PSDM, PSTM, CSPD, etc.).
- If a method uses both amplitude and phase of acoustic wave, then these method can be called **vector-based method** (RTH) and finally,
- if a method uses tensor information of elastic medium, then this type of seismic imaging method can be called **tensor-based method** (Tensor Reverse Time Holography - TRTH).

# Examples

The four case studies of RTH data processing are presented below for different geological region, dimension (2D, 3D) and voxel sizes. Everywhere the step between receivers is 25 m, between sources - 50m, time sampling - 2 milliseconds.

The all attribute estimations are calculated using HPC 50 Teraflops.

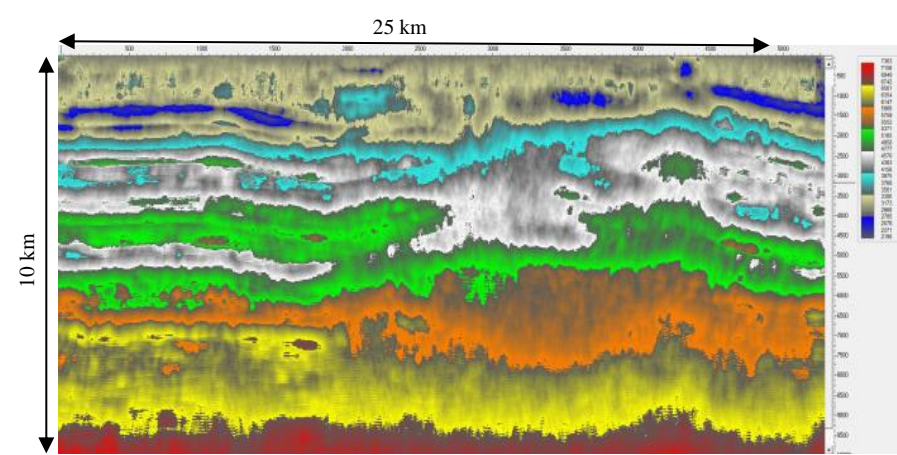
The background velocity model is the simple linear gradient:

for 2D case study #1- from 3 km/s up to 7 km/s (for the depth 10 km) -North Arctic (4 sl.)

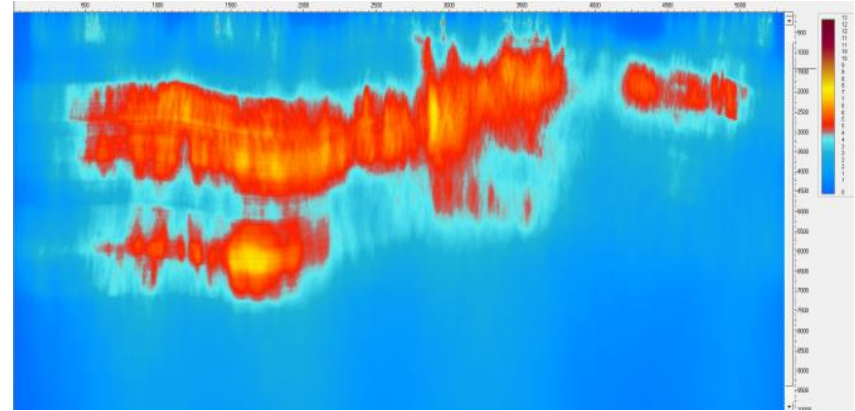
for 2D case study #2 - from 3 km/s up to 3.75 km/s (for the depth 3 km)-Europe, Baltic (1sl.)

for 3D case study #3 - from 5 km/s up to 5.2 km/s (for the depth 2 km)- Eastern Siberia (1sl.)

for 3D case study #4 - from 5 km/s up to 5.2 km/s (for the depth 2 km)- Eastern Siberia (5sl.)

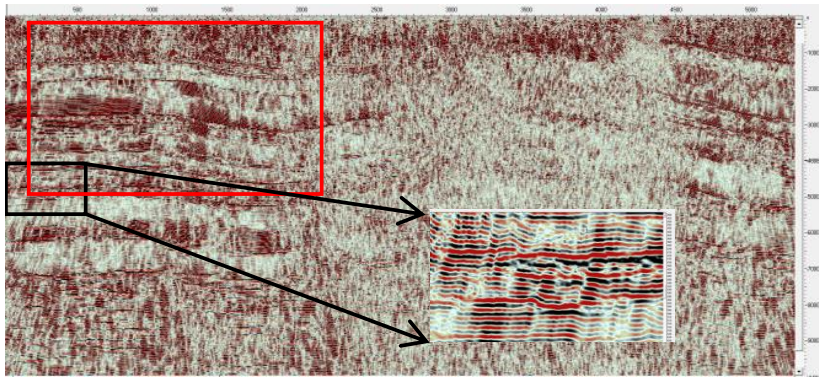


a



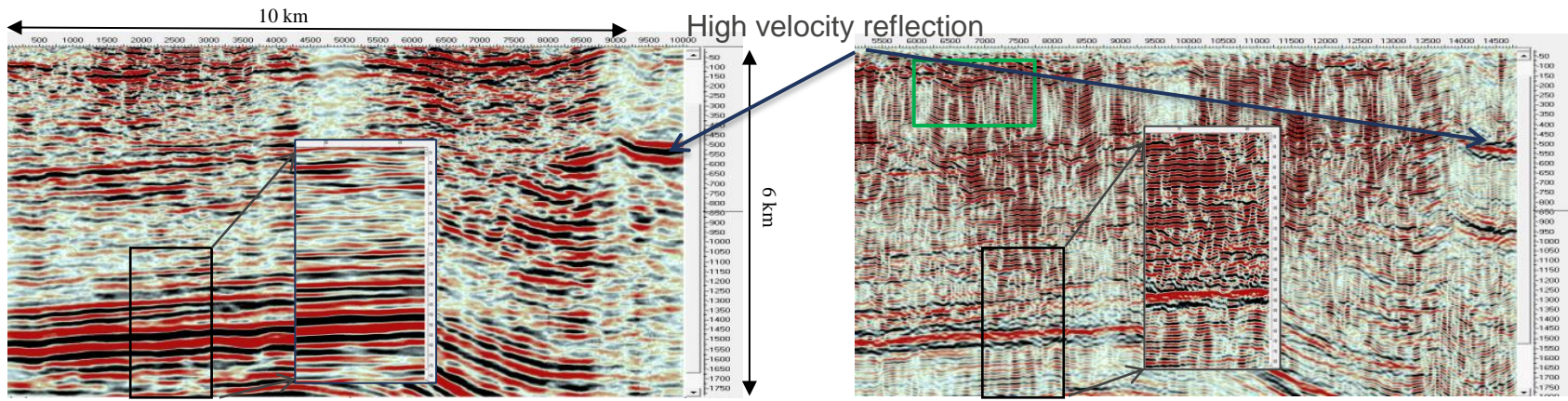
b

## 2D Case Study #1. High resolution RTH attributes. Long profile. Great depth.



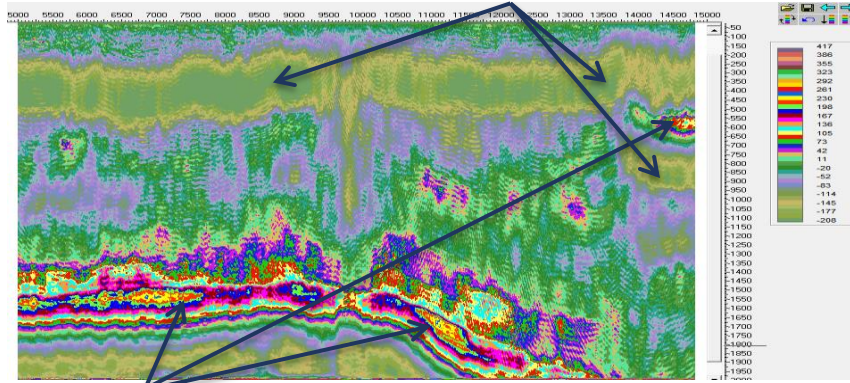
c

Figure 7: Long seismic profile. Voxel size is 25x5 m.  
 a - RTH velocity - from 2190 m/s (bottom) to 7363 m/s (top)  
 b - Scattering Index (Diffractivity)  
 c - RTH Velocity Residual



a Low velocity

b



High velocity c

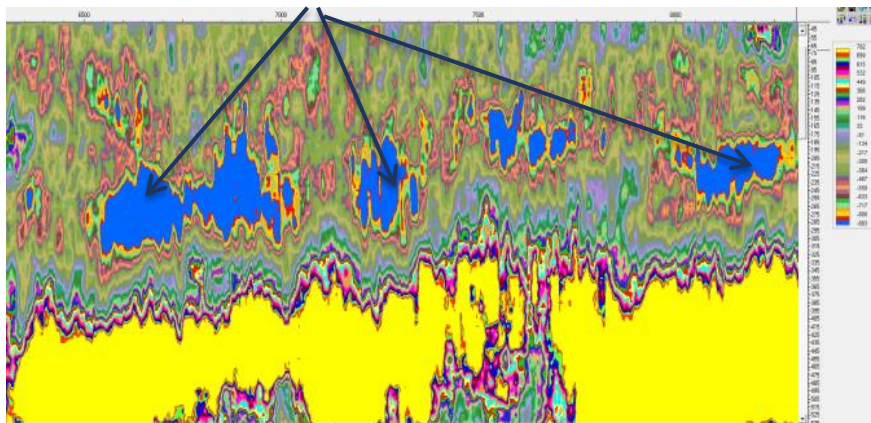
## 2D Case Study #1. Comparison PSDM & RTH. Zooming red box.

Figure 8: Zooming the red box at Fig. 6c. Voxel size is 5x5 m.

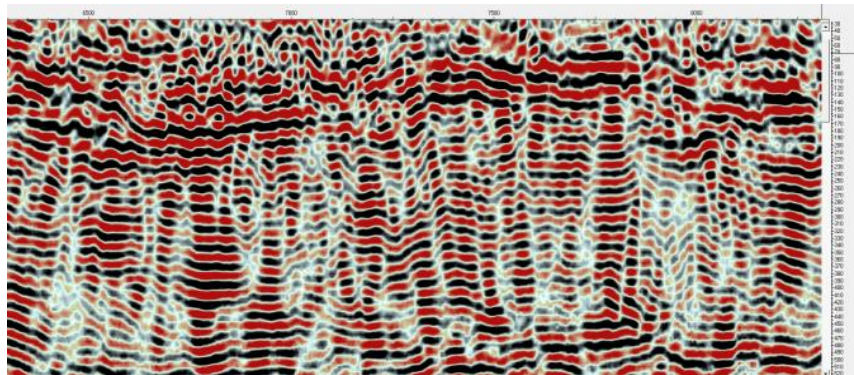
- a - The Kirchhoff Depth Migration
- b- RTH Velocity Residual
- c- RTH velocity perturbation from -208 m/s (bottom) to 417 m/s (top) (c)

The spatial resolution of RTH migration images is 2-3 times higher compared to conventional depth migration before summation

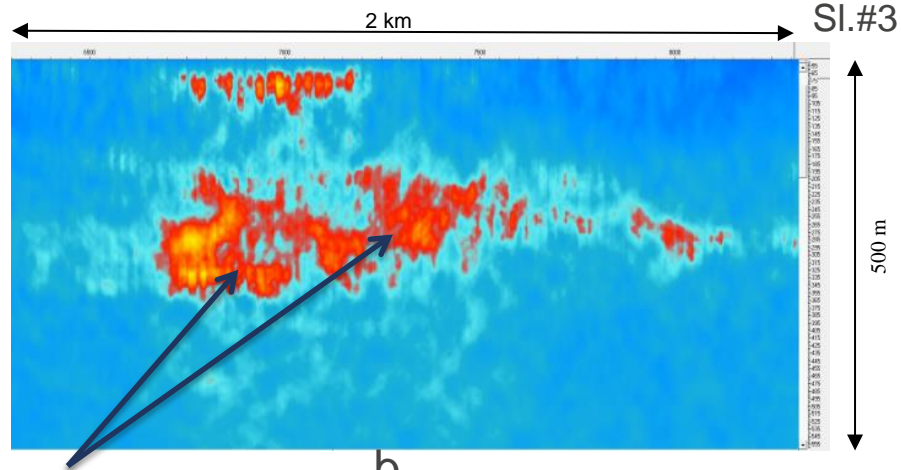
High velocity inclusions



a



c



Natural fracture

## 2D Case Study #1. High resolution RTH attributes for upper part of the depth section. Zooming green box.

- Figure 9: Zooming the green box at Fig. 7 (b). Voxel size is 5x5 m.
- a- The RTH Velocity Perturbation from -883 m/s (bottom) to 782 m/s (top)
  - b- Scattering Index (Diffractivity)
  - c- RTH Velocity Residual

# 2D Case Study #1. RTH velocity for Geosteering for horizontal drilling

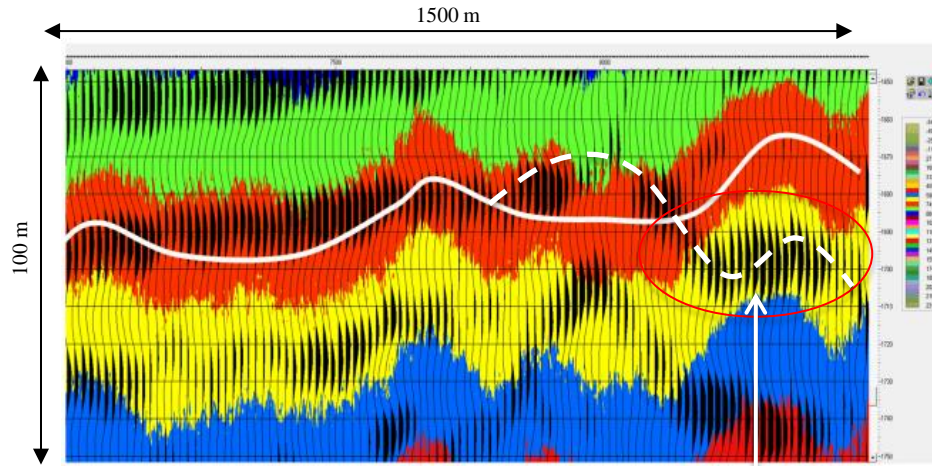


Figure 10: The RTH Velocity with RTM wiggle. Voxel size is 2x2 m. White line is proposed trajectory for horizontal well.

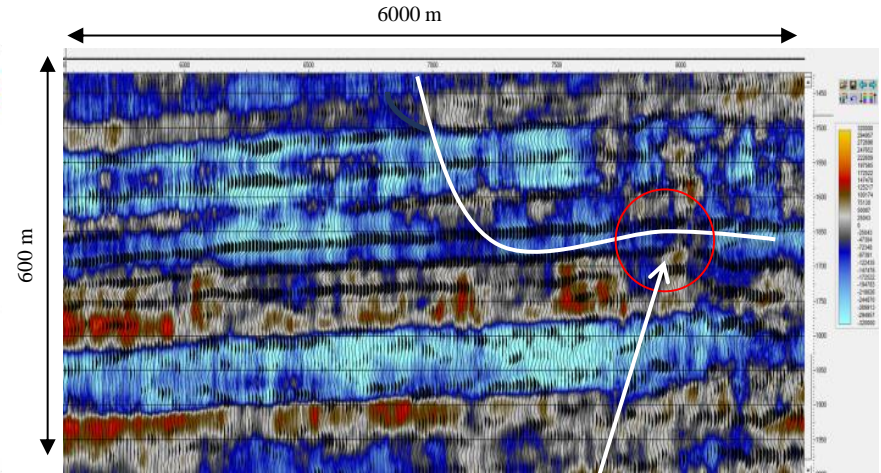


Figure 11: RTH AVO Poison attribute. Voxel size is 2x2 m.

Change properties

According RTM - down

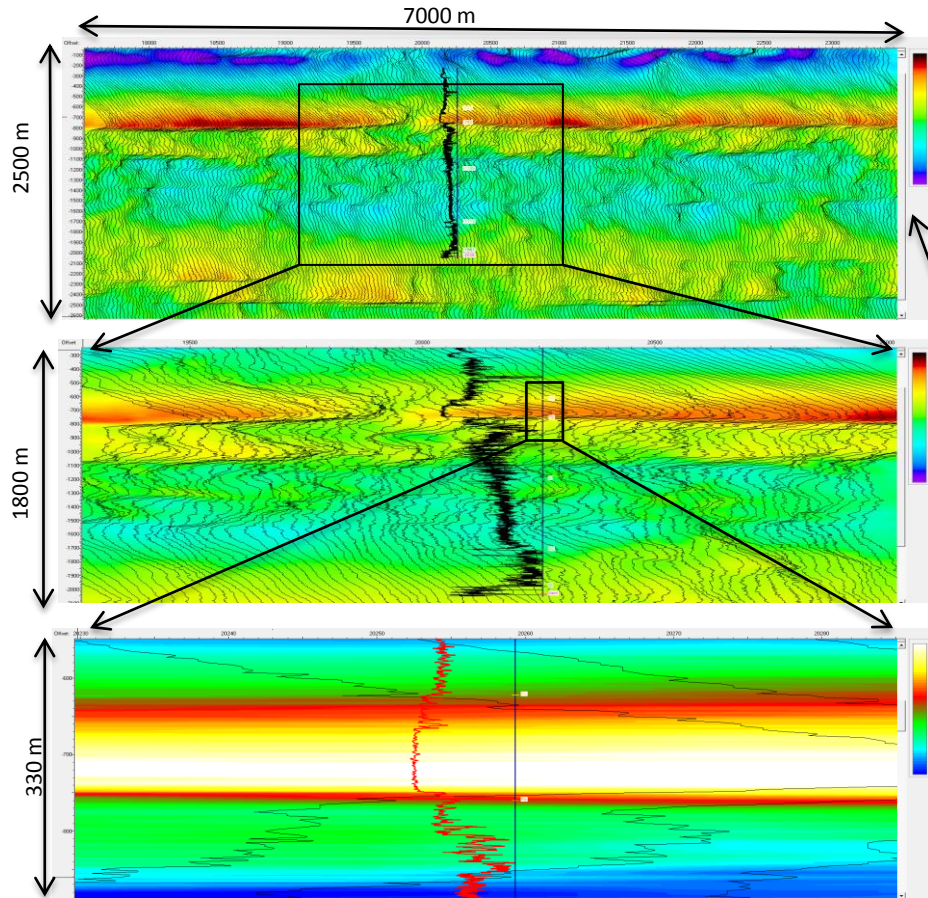


RTH Geosteering

Conventional RTM Geosteering

# 2D Case Study #2. Enhanced spatial resolution of seismic attributes.

## Zooming cascade

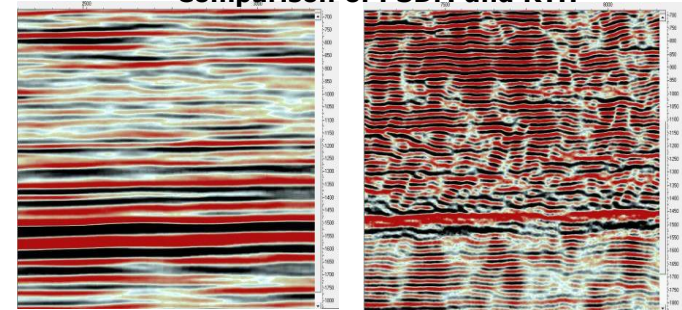


**The spatial resolution of migration images is 2-3 times higher compared to conventional depth migration before summation**

- Ultra high resolution (up to 2 meter)
- Ensuring efficient comparison of RTH attributes with GIS data due to the equivalent spatial resolution of RTH and GIS data

2D RTH velocity with overlay of the GR curve. The size of the velocity pixel is 12.5x2.5 m. The dimension of the region is 7.0x2.5 km. The red color of the palette is high-velocity deposits of Perm. Baltic Syncline.

### Comparison of PSDM and RTH

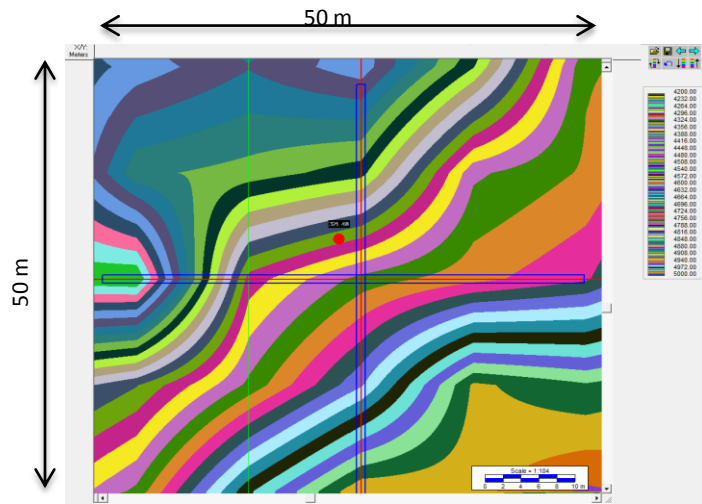


**Kirchhoff  
Depth Migration**

**RTH  
Depth Migration**

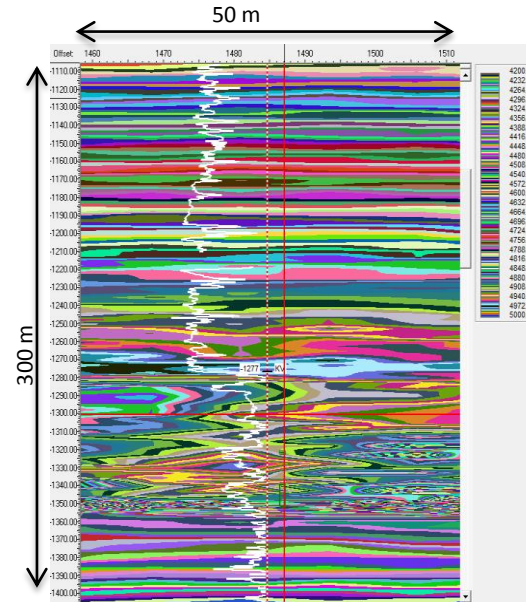


# 3D Case Study #3. 3D Velocity tomography with a spatial resolution 2.5 meter and high number of color bar

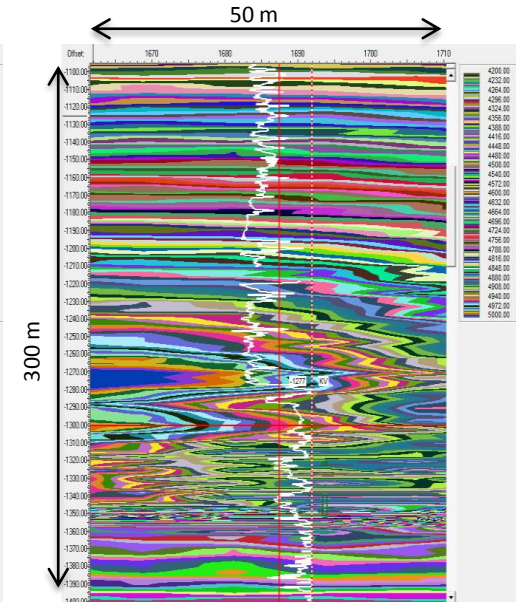


This slide demonstrates the scale resolution of RTH-approach, which is same as the scale resolution of logging data

The small horizontal slice of a 3D RTH velocity cube at a depth of 1300 m. The spatial size of the velocity voxel is 12.5x12.5x2.5 m. The dimension of the slice is 50x50 meters. Velocity scale - from 4200 to 5000 m / s. Eastern Siberia.

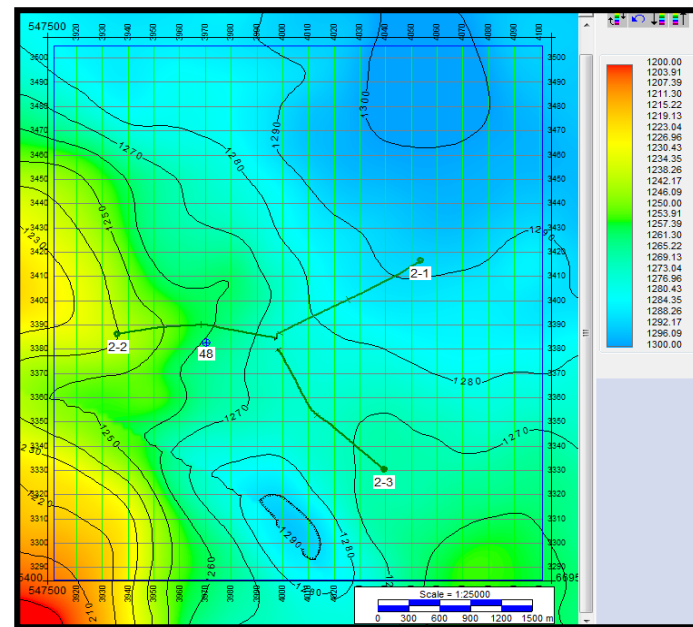
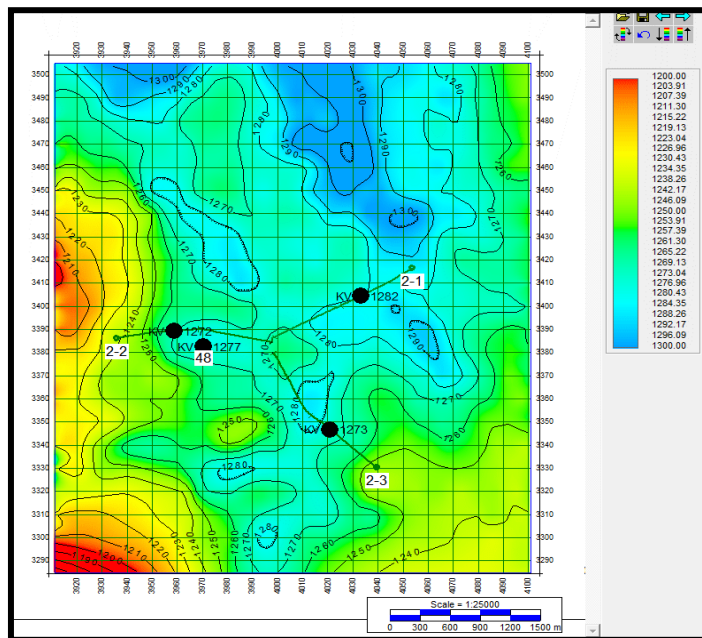


Vertical section of a RTH velocity cube. Inline, dimension is 50x300 m. Depths are from 1100 up to 1400 m. Velocity scale is from 4200 up to 5000 m/s. The white line is the Gamma Ray (GR) log.



Vertical section of a RTH velocity cube. Crossline, dimension is 50x300 m. Depths are from 1100 up to 1400 m. Velocity scale is from 4200 up to 5000 m/s. The white line is the Gamma Ray (GR) log.

# 3D Case Study #4. Comparison of KV horizon structural map constructed using the velocity-based RTH approach with the conventional PSDM map



RTH map, m

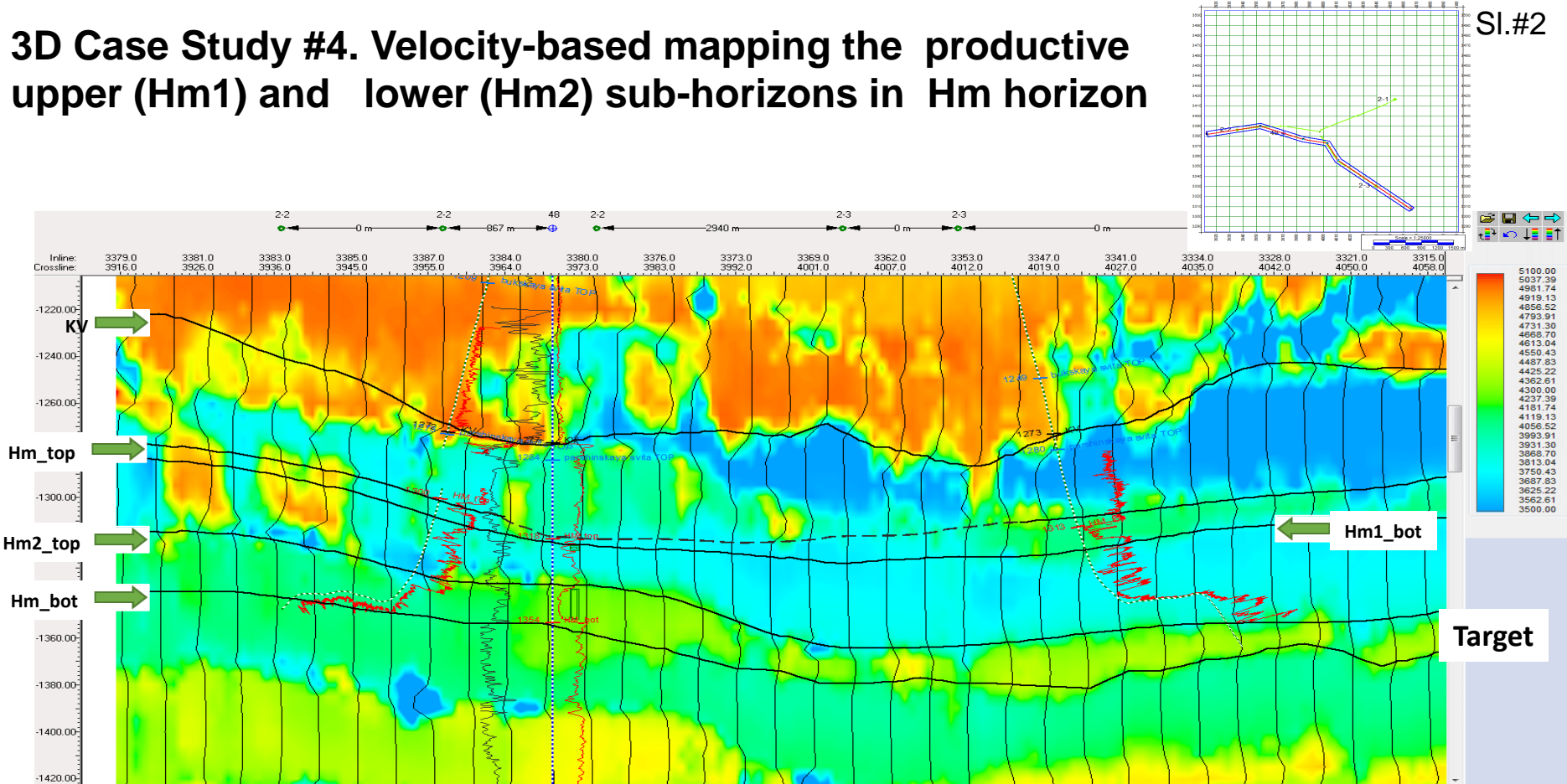
PSDM map, m

Black dots on the map -  
KV's depth by inclinometry

Well #	Depth, well (m)	Depth, RTH map (m)	Error (m)
48	1277	1272	5
2-1	1282	1280	2
2-2	1272	1271	1
2-3	1273	1274	1

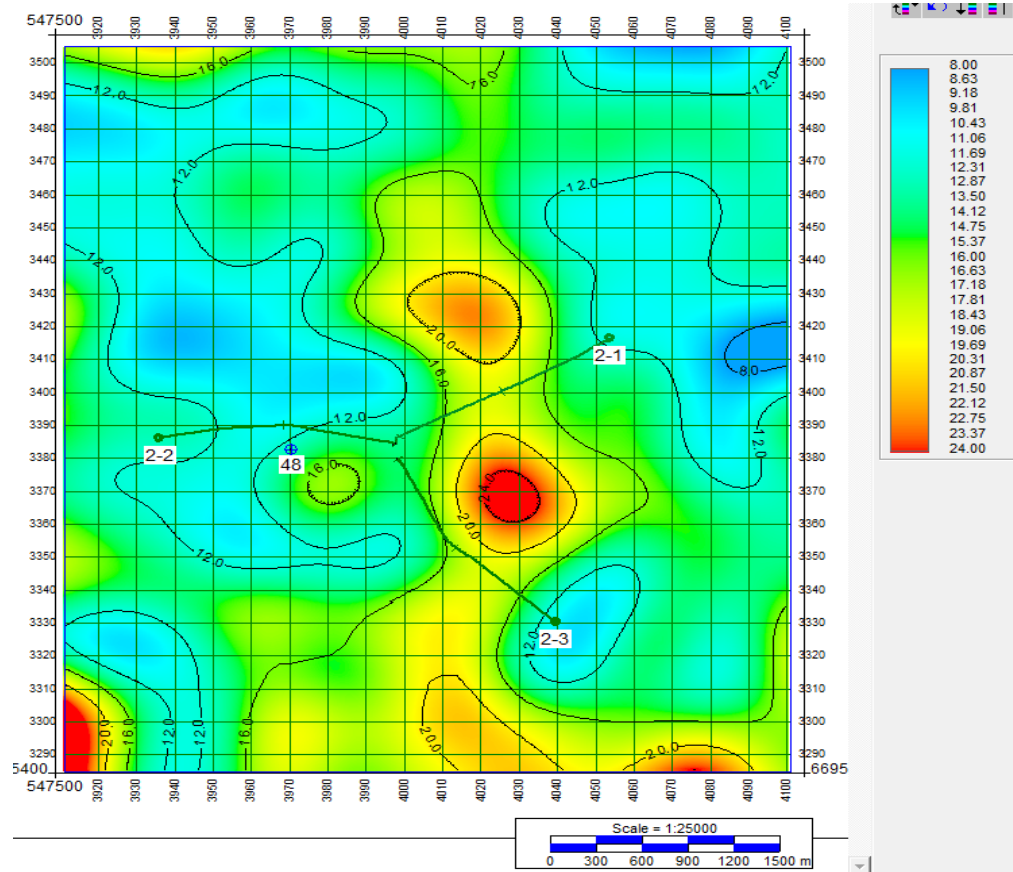
# 3D Case Study #4. Velocity-based mapping the productive upper (Hm1) and lower (Hm2) sub-horizons in Hm horizon

Sl.#2

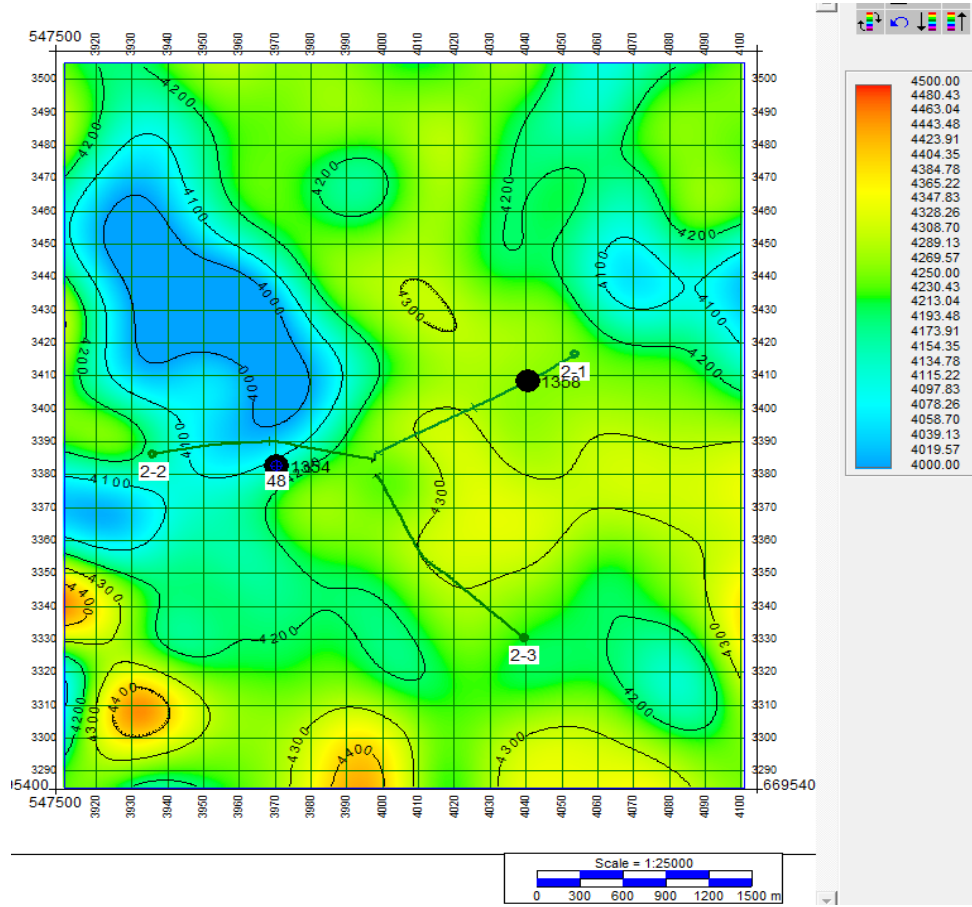


Scale RTH-velocity m/s, wiggle- RTH-velocity. The spatial size of the velocity voxel is 12.5x12.5x2.5 m. Eastern Siberia.

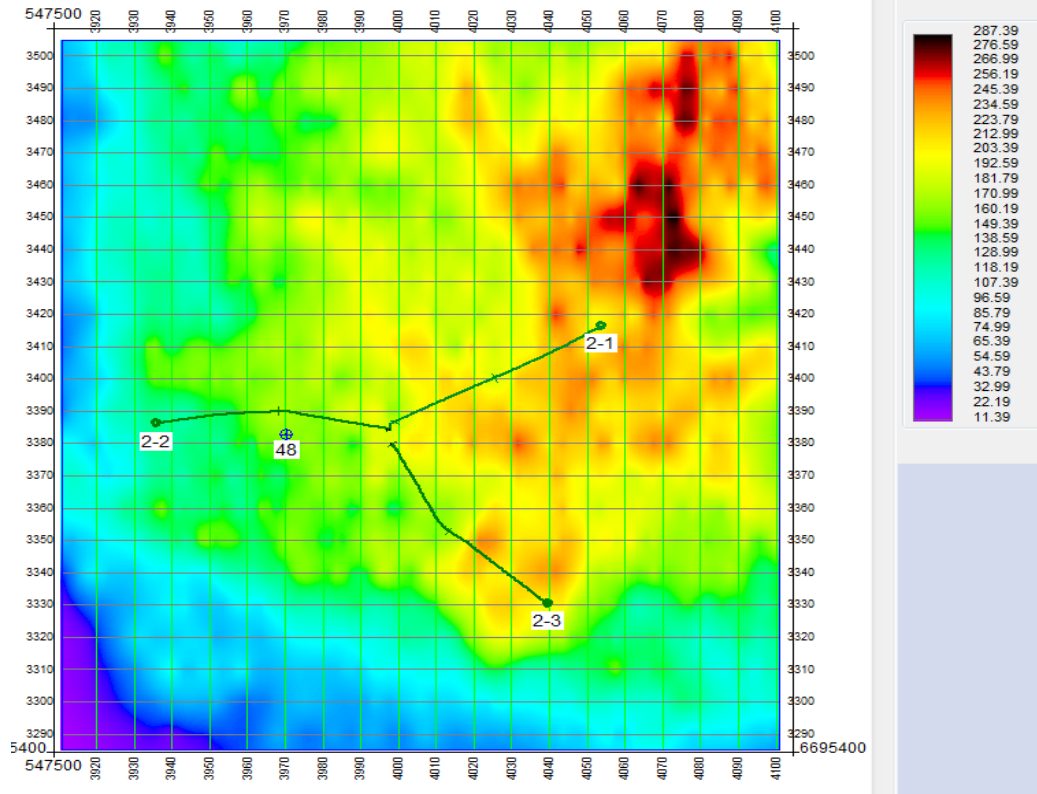
# 3D Case Study# 4. Thickness map of the lower productive Hm2 sub-horizon in meters



# 3D Case Study# 4. Velocity map of the productive Hm2 sub-horizon in meters per second



# 3D Case Study# 4. Fracture map of the productive Hm2 sub-horizon in relative units



# Conclusions

- The high-resolution velocity model estimation by the Reverse Time Holography method is proposed.
- It is shown that the one of the new depth seismic attribute, which is called the RTH Velocity Residual and which is based on the high-precision velocity model estimation has a spatial resolution of more than two-three times higher than Kirchhoff's depth migration.
- The data processing examples for differ types of pixel size starting from 2 meters are presented.
- Example of using high-resolution RTH-velocity for constructing maps of productive horizons and their attributes is presented.
- The new voxel-based classification of the seismic imaging methods based on the essence of formal operations on wave data at each point of the medium is proposed.

# Acknowledgments

The authors thank colleagues and friends Sergey Sergeev, Maksim Kozlov and Svetlana Shevchenko for help and useful participation. This work is supported by the Russian Science Foundation under grant 16-11-10027.

# REFERENCES

- Baysal, E., D. D. Kosloff, and J. W. C. Sherwood, 1983, Reverse time migration: Geophysics, 48, 1514–1524, <https://doi.org/10.1190/1.1441434>
- Fitzpatrick Gerald, Mueller Rolf K., Steinberg Ron F., and Gupta Ray R., 1972, Seismic Holography, The Journal of the Acoustical Society of America 51, 119 (1972); <https://doi.org/10.1121/1.1981339>
- Gabor, D. A new microscopic principle. Nature 161, 777\_778 (1948).
- Erokhin G., Pestov L., Danilin A., Kozlov M., and Ponomarenko D., 2017, Interconnected vector pairs image conditions: New possibilities for visualization of acoustical media, 2017, SEG Technical Program Expanded Abstracts 2017: 4624-4629., <https://doi.org/10.1190/segam2017-17587902.1>
- Erokhin Gennady, Danilin Aleksandr, and Maksim Kozlov, 2018a, Extension of the common image gathers by VPRM method. SEG Technical Program Expanded Abstracts 2018: pp. 4438-4442.
- Erokhin G., Danilin A. and M. Kozlov, 2018b, Visualization of Ultra-Weak Diffractors based on Vector Pair RTM, 80th EAGE Conference and Exhibition 2018, <https://doi.org/10.3997/2214-4609.201801648>
- Erokhin G., Reverse Time Holography Approach based on the Vector Domain Common Image Gathers, 2019, SEG Technical Program Expanded Abstracts 2019: 4107-4111., <https://doi.org/10.1190/segam2019-3201622.1>
- McMechan, G. A., 1983, Migration by extrapolation of time-dependent boundary values: Geophysical Prospecting, 31, 413–420, <https://doi.org/10.1111/j.1365-2478.1983.tb01060.x>.
- Robinson Enders A, 2018, Extended resolution: Neidell is right, THE LEADING EDGE, January 2018, pp.33-36. <https://doi.org/10.1190/tle37010033.1>.
- Tarantola, A., 1984, Inversion of seismic reflection data in the acoustic approximation: Geophysics, 49, 1259–1266. <https://dx.doi.org/10.1190/1.1441754>
- Virieux, J., and Operto, S., 2009, An overview of full-waveform inversion in exploration geophysics: GEOPHYSICS, 74, WCC1–WCC26. <https://dx.doi.org/10.1190/1.3238367>
- Yoon, K., and K. J. Marfurt, 2006, Reverse-time migration using the Poynting vector: Exploration Geophysics, 37, 102–107.



# Thanks!

[egn@rthtech.com](mailto:egn@rthtech.com)

